Marine Biotechnology (2020) 22:1–18
https://doi.org/10.1007/s10126-019-09932-8

ORIGINAL ARTICLE

Fine Mapping of the High-pH Tolerance and Growth Trait-Related Quantitative Trait Loci (QTLs) and Identification of the Candidate Genes in Pacific White Shrimp (*Litopenaeus vannamei*)

Wen Huang[1,2] · Chuhang Cheng[1,3] · Jinshang Liu[1,4] · Xin Zhang[1,3] · Chunhua Ren[1,3] · Xiao Jiang[1] · Ting Chen[1] · Kaimin Cheng[1,5] · Huo Li[1,4] · Chaoqun Hu[1,2,3]

Received: 15 June 2019 / Accepted: 12 August 2019 / Published online: 22 November 2019

Abstract

High-pH tolerance and growth are important traits for the shrimp culture industry in areas with saline-alkali water. In the present study, an F1 full-sib family of Pacific white shrimp (*Litopenaeus vannamei*) was generated with a new "semidirectional cross" method, and double-digest restriction site-associated DNA sequencing (ddRAD-Seq) technology was applied to genotype the 2 parents and 148 progenies. A total of 3567 high-quality markers were constructed for the genetic linkage map, and the total map length was 4161.555 centimorgans (cM), showing 48 linkage groups (LGs) with an average interlocus length of 1.167 cM. With a constrained logarithm of odds (LOD) score ≥ 2.50, 12 high-pH tolerance and 2 growth (body weight) QTLs were located. *L. vannamei* genomic scaffolds were used to assist with the detection of 21 stress- and 5 growth-related scaffold genes. According to the high-pH transcriptome data of our previous study, 6 candidate high-pH response genes were discovered, and 5 of these 6 genes were consistently expressed with the high-pH transcriptome data, validating the locations of the high-pH tolerance trait-related QTLs in this study. This paper is the first report of fine-mapping high-pH tolerance and growth (body weight) trait QTLs in one *L. vannamei* genetic map. Our results will further benefit marker-assisted selection work and might be useful for promoting genomic research on the shrimp *L. vannamei*.

Keywords *Litopenaeus vannamei* · ddRAD-Seq · QTL · High-pH stress · Growth trait

Wen Huang and Chuhang Cheng contributed equally to this work.

Electronic supplementary material The online version of this article (https://doi.org/10.1007/s10126-019-09932-8) contains supplementary material, which is available to authorized users.

✉ Wen Huang
huangwen@scsio.ac.cn

✉ Chaoqun Hu
hucq@scsio.ac.cn

[1] CAS Key Laboratory of Tropical Marine Bio-resources and Ecology (LMB)/Guangdong Provincial Key Laboratory of Applied Marine Biology (LAMB), South China Sea Institute of Oceanology, Chinese Academy of Sciences, Guangzhou 510301, China

[2] Institution of South China Sea Ecology and Environmental Engineering (ISEE), Chinese Academy of Sciences, Guangzhou 510301, China

[3] University of Chinese Academy of Sciences, Beijing 100049, China

[4] Guangdong Jinyang Biotechnology co. LTD, Maoming 525027, China

[5] Yuehai Feed Group co., LTD, Zhanjiang 524017, China

Introduction

The Pacific white shrimp, *Litopenaeus vannamei* (*L. vannamei*), is famous worldwide as a high-quality food in the human diet (FAO 2012). With the high economic value and good stress resistance of this species (Li et al. 2007, Wang et al. 2013a, b), *L. vannamei* has become one of the most important aquatic species for culturing, and *L. vannamei* farming areas have been widely introduced in nonnative environments worldwide (Huang et al. 2018). Total shrimp production reached 4 million tons, and the total output value achieved 24 billion US dollars in 2016 (Yu et al. 2019). Advances in shrimp breeding projects might further promote the high economic value of the shrimp culture industry.

Soil salinization significantly impacts crop yields and poses a threat to regional human life; therefore, the strategy of reusing and transferring saline-alkali lands as cultivated resources is becoming imperative (Li et al. 2014; Wang et al. 2017; Huang et al. 2018). The development of aquaculture industries in saline-alkali water areas, including inland lakes,

rivers, and marine coasts in China, has been thought to be an effective method for taking full advantage of these territorial resources (Liang et al. 2013; Liu et al. 2016) and has economic (production of saline-alkali water reached USD$1.14 million) (Liu et al. 2016) and environmental (the top pH value of the saline-alkali lands dropped from 9.01 to 8.56) (Xue 2018) value in the Hebei and Shaanxi Provinces of China. *L. vannamei* is one of the most important aquatic species for culturing in saline-alkali water areas in China (Luan et al. 2003; Liu et al. 2008; Zhang 2016). However, compared with the farming of *L. vannamei* under normal seawater conditions, the immunity and production of the shrimp might be weakened when the species is cultured in high-pH environments (Li and Chen 2008; Wang et al. 2009; Huang et al. 2018). The high-pH tolerance trait of the shrimp has become an important economic trait for the breeding and culturing industries.

The development of marker-assisted selection (MAS) has substantially accelerated genetic breeding work (Yue 2014; Abdelrahman ElHady et al. 2017; Li et al. 2017; Yu et al. 2019; Li et al. 2019). Most targeted traits of species are governed by multiple genes or loci, and quantitative trait loci (QTLs) mapping with dense genetic linkage maps is employed to reveal the locations of the trait-related genes (Yue 2014; Das et al. 2015; Wan et al. 2017; Li et al. 2017; Kong et al. 2019; Li et al. 2019). Single nucleotide polymorphism (SNP) markers, which represent the most abundant source of variation in the genome, are increasingly utilized for the construction of high-density genetic linkage maps (Lien et al. 2011; Shao et al. 2015; Wan et al. 2017). High-resolution genetic maps with 12,712 high-confidence SNPs and 24 consensus linkage groups (LGs) were constructed for the Japanese flounder (*Paralichthys olivaceus*, *P. olivaceus*), and 9 positive QTLs and 4 major genes for *Vibrio anguillarum* disease resistance were detected (Shao et al. 2015). Yu et al. (2015) used a total of 6146 high-quality SNP markers for QTL mapping, and an average marker distance of 0.7 cM was obtained for the linkage map (Yu et al. 2015).

With the development of next generation sequencing (NGS) technology, high-throughput marker development and genetic map construction has become possible to finely map trait-related QTLs (Shao et al. 2015, Wan et al. 2017). In recent years, many advanced methods for mapping trait-related QTLs have been developed, such as genome-wide association studies (GWAS) (Abdelrahman ElHady et al. 2017), expression quantitative trait loci (eQTLs) (Imprialou et al. 2017), specific-locus amplified fragment sequencing (SLAF) (Miller et al. 2007), genotyping-by-sequencing (GBS) (Baird et al. 2008), and restriction site-associated DNA sequencing (RAD-seq) (Sun et al. 2013). In particular, as a reliable, affordable method to reduce genomic complexity, RAD-Seq has been very useful for SNP discovery and genotyping (Berthier-Schaad et al. 2007; Rowe et al. 2011; Wang et al. 2012; Shao et al. 2015; Fu et al. 2016; Wan et al. 2017). RAD-Seq technology has now been applied for the genetic study of various aquatic species, such as *P. olivaceus* (Shao et al. 2015), *Hypophthalmichthys nobilis* (Fu et al. 2016), *Megalobrama amblycephala* (Wan et al. 2017), *Trachinotus blochii* (Zhang et al. 2018), *Larimichthys crocea* (Kong et al. 2019), and *Oreochromis* spp. (Li et al. 2017; Li et al. 2019).

In previous studies on *L. vannamei*, the genetic mechanism of growth traits has been elucidated (Andriantahina et al. 2013; Yu et al. 2015, Yu et al. 2019), but few genes have been identified in association with growth traits (Yu et al. 2019). Further genetic studies on growth-related traits in this species are still needed. The high-pH tolerance trait of the shrimp is becoming an important economic trait for industrial breeding and culturing in saline-alkali water areas; however, the stress response QTLs are still unknown. In the present work, double-digest restriction site-associated DNA sequencing (ddRAD-Seq) technology was applied to genotype an F1 full-sib family of *L. vannamei*, and a high-resolution genetic map was constructed with high-quality SNP markers. High-pH tolerance and growth (body weight) trait-related QTLs were detected, high-pH response and growth-related candidate genes were discovered, and real-time PCR was carried out to validate the candidate high-pH response genes. Our results will further benefit MAS work and might be useful for promoting genomic research on the shrimp *L. vannamei*.

Materials and Methods

Shrimp Full-Sib Family Production

An F1 full-sib shrimp family was produced by inner species crossing at JingYang Tropical Biology Co., LTD in Maoming, Guangdong, China (August, 2017). The female shrimp were selected from the inbred line called "*L. vannamei* ZhongKe No.1" (a shrimp variety in China, variety registration no. GS-01-007-2010), and the candidate male shrimps were obtained from a commercial shrimp termed "Zheng Da." According to the propagation characteristic (open thelycum) of *L. vannamei*, mating a single mature male shrimp with a mature female was difficult, and a full-sib shrimp family was thus produced with a new "semidirectional cross" method according to the following steps. A fertile female shrimp (containing yellow shrimp eggs) (Supplementary Fig. 1a) was placed in a seawater mating pond (5 m^2, 1 m height) that contained 7–15 fertile male shrimps, whose spermatophores were packed with white spermatia (Supplementary Fig. 1b). The male shrimps in the mating pond took turns to chasing the female until mating occurred, then, the female shrimp whose thelycum contained the white spermatia (Supplementary Fig. 1c) was removed. The mated female shrimp was reared in an isolation tank (round, 70 cm in height, volume ≤ 1000 L) for spawning

and served as the female parent of the F1 full-sib family. The male parent of the F1 full-sib family was visually determined by determining based on which male showed an empty spermatophore (without packed spermatium) (Supplementary Fig. 1b, d), as naturally, only one male shrimp could mate with the female shrimp. The F1 full-sib progenies were first nursed in the tank for 15 days, and the full-sib shrimps were then moved to an indoor culturing pond (5.0 m in length, 6.0 m in width, and 1.2 m in height) for further rearing.

High-pH Challenges and Preparation of the Shrimp Samples

After being reared in the culturing pond for 40 days, 35 of the full-sib progenies were randomly selected and treated in a high-pH gradient environment (gradient pH values of 8.1, 8.3, 8.5, 8.7, 8.9, 9.1, 9.3, 9.5, and 9.7) for 48 h. The pH values were maintained with Na_2CO_3 and $NaHCO_3$ solutions according to the description by Huang et al. (2018). The survival statuses of the shrimp were evaluated by observing their ability to move spontaneously or after gentle prodding (Huang et al. 2017). The dead individuals were collected, and the endurance times were recorded for each pH level. The high-pH stress was determined by evaluating the number of survivors in each high-pH treatment group.

A total of 148 full-sib progenies were randomly selected from nearly 5000 whole full-sib family numbers in the rearing pond and treated in the stress high-pH environments. Afterward, the dead shrimps were collected and weighed. The data regarding the endurance times under the stress of the high-pH environment (high-pH tolerance trait, HP) and body weight (body weight, growth trait, BW) were collected. The muscle tissues of 2 parents and 148 offspring were separated for the extraction of genomic DNA, and the experiments were conducted with the TIANGEN Marine Animal DNA extraction kit (TIANGEN, Beijing, China) according to the manufacture's protocol. The concentration of total DNA was determined with a NanoDrop 1000 spectrophotometer (NanoDrop, Wilmington, DE, USA), and the quality of each DNA sample was evaluated by gel electrophoresis (Yu et al. 2015).

RAD Library Construction and Sequencing

Genomic DNA from 2 parents and 148 offspring was used to construct the 150 *L. vannamei* ddRAD libraries (October 2017) using protocols described by Peterson et al. (2012) and Sun et al. (2017). Briefly, the DNA from each shrimp sample was double-digested using the restriction enzymes *Eco*RI and *Nla*III (New England Biolabs, Ipswich, MA, USA) (Yu et al. 2015). Then, the digested samples were purified using a Qiagen MinElute Reaction Cleanup Kit (Qiagen, Valencia, CA, USA). The fragments were then ligated to adapters that included unique 4- to 8-bp multiplex identifiers (MIDs) that were used to distinguish each individual. The samples were pooled, size-selected (400 to 600 bp) on an agarose gel and subsequently purified with a Qiagen MinElute Gel Purification Kit. The paired-end (150 bp) sequencing of the ddRAD products was performed on an Illumina HiSeq 2500 platform (Illumina, Inc., San Diego, CA, USA).

SNP Discovery and Genotyping

The Illumina short reads that lacked the sample-specific MIDs and the expected restriction enzyme motifs were discarded. The raw data were then filtered using Trimmomatic software (v0.32) (Bolger et al. 2014) in three steps: removal of adapters; removal of reads with bases from the start or end of a read with a quality threshold below 3; and scanning reads with a 4-bp sliding window, removing those with an average Phred quality per base below 20 (Sun et al. 2017). The STACKS (v1.41) (Catchen et al. 2013) pipeline was employed for de novo assembly of the loci and for SNP discovery. The Ustacks program was used to cluster the enzyme cutting sequences of each individual, and the Cstacks program was applied to identify the congruent loci and make the alleles in the parental data uniform. The Sstacks program was utilized to compare the progeny and parent loci, confirming the genotype of each progeny locus; and the Genotype program was utilized to proofread the genotype data. The following parameters were used:

Ustacks: -t gzfastq -i -m 3 -M 9 -p 15 -d -r –f –o
Cstacks: -b 1 –o –s –n 2 –p 15
Sstacks: -b 1 –c –p 15
Genotype: -b 1 –P -r 1 -c -s -t CP

The miss rates (number of samples with no genotype information/number of total samples) were less than 10%, and biallelic SNPs were used to avoid sequencing errors and to advance the segregation analysis (Sun et al. 2017; Lu et al. 2016). The sequencing depth of the SNP loci was no less than 5.

Linkage Map Construction

Only biallelic SNPs were introduced to construct the genetic linkage map, and the SNP genotypes were defined as follows: (1) SNPs that were heterozygous in the maternal parent (lm) and homozygous in the paternal parent (ll); (2) SNPs that were heterozygous in the paternal parent (np) and homozygous in the maternal parent (nn); and (3) SNPs that were heterozygous in the maternal and paternal parent (hk) (Lu et al. 2016). Biallelic SNPs that presented significant segregation

distortion in the χ^2 goodness-of-fit tests (chi-square test, $P < 0.05$) were also eliminated in the linkage analysis (Liu et al. 2017). LG assignments were conducted with JoinMap 4.1 software (Stam 1993) using a logarithm of odds (LOD) score ≥ 6.0. A pseudo-testcross strategy (a mapping population was developed by hybridizing two unrelated highly heterozygous parents to produce a set of F1 progeny) was utilized to construct the linkage map (Shao et al. 2015; Sun et al. 2017). The regression mapping algorithm and Kosambi's mapping function were used for map construction with the following settings: Rec = 0.4, LOD = 1.0, and Jump = 5. The genetic distance of 30 cM was set as the longest gap between two markers in one LG. The resulting linkage maps were drawn using R software (version of R x64 3.5.2, https://www.r-project.org/) with the package LinkageMapView (Ouellette et al. 2018).

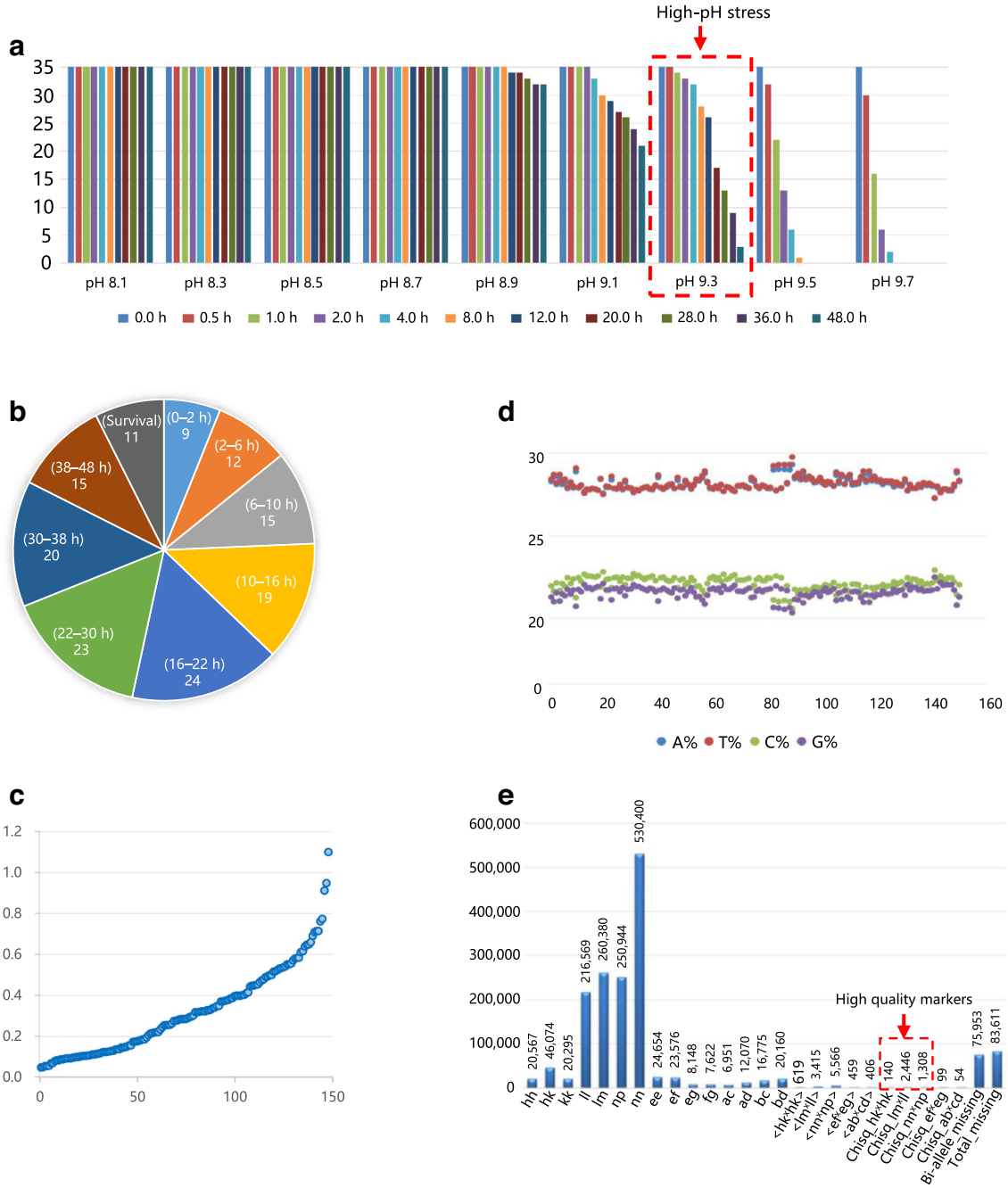

Fig. 1 Information on the experimental and RAD-Seq libraries. **a** High-pH challenges in gradient high-pH environments for 48 h; the high-pH stress condition of the full-sib family is indicated. **b** Summary of the high-pH tolerance data of the full-sib offspring. **c** Summary of the body weight data of the full-sib offspring. **d** Quality control of the RAD-Seq libraries. The X axes represent the base position along the reads. The Y axes represent the base content percentages. **e** Summary of the SNP markers; high-quality markers are enclosed in a box

QTL Mapping

QTL mapping of the HP and BW traits was performed with MapQTL 5.0 software (Van Ooijen 2011). The Multiple QTL Mapping (MQM) program was used to detect the QTL region and calculate the percentage of explained phenotypic variance (Jansen and Stam 1994); an LOD ≥ 2.50 was set for the trait-related QTL regions. A mapping step size of 1 cM and five neighboring markers were used in the QTL analysis (Louro et al. 2016; Liu et al. 2017). The genome-wide LOD threshold (significance level) or group-wide LOD threshold (suggestive level) was determined in MapQTL5.0 by a Permutation Test on the basis of 1000 permutations with a confidence interval of 95% (Piepho 2001; Lu et al. 2016).

Identification of the Candidate High-pH Response and Growth-Related Genes

To further reveal the high-pH response and growth-related genes, the tag sequences of the HP and BW QTL markers

Table 1 Summary information of the linkage groups for the shrimp full-sib family

Linkage group	Number of markers	Genetic length (cM)	Average interval (cM)	Largest gap/length (cM)
LG 1	166	165.922	1.000	9.726~35.900/26.174
LG 2	183	154.313	0.843	120.361~148.372/28.011
LG 3	61	154.002	2.525	119.507~141.590/22.083
LG 4	91	152.002	1.670	106.191~133.530/27.339
LG 5	70	151.135	2.159	0.000~28.177/28.177
LG 6	99	148.734	1.502	32.146~59.721/27.575
LG 7	119	136.537	1.147	115.308~136.537/21.229
LG 8	99	135.317	1.367	23.664~50.546/26.882
LG 9	96	133.586	1.392	2.228~14.263/12.035
LG 10	85	129.095	1.519	0.682~30.146/29.464
LG 11	133	128.262	0.964	18.444~42.983/24.539
LG 12	112	124.096	1.108	20.629~44.230/23.601
LG 13	77	120.769	1.568	76.061~94.227/18.166
LG 14	50	118.870	2.377	0.000~22.968/22.968
LG 15	90	115.632	1.285	92.317~113.356/21.039
LG 16	110	109.889	0.999	86.841~107.652/20.811
LG 17	124	108.422	0.874	12.212~23.072/10.860
LG 18	103	101.313	0.984	71.244~85.946/14.702
LG 19	107	101.097	0.945	76.524~99.637/23.113
LG 20	72	98.369	1.366	72.723~87.758/15.035
LG 21	105	95.948	0.914	0.000~15.805/15.805
LG 22	87	93.684	1.077	50.577~65.861/15.284
LG 23	33	90.607	2.746	32.311~57.841/25.530
LG 24	84	85.396	1.017	0.000~15.791/15.791
LG 25	51	81.410	1.596	10.193~28.854/18.661
LG 26	51	77.351	1.517	36.609~50.643/14.034
LG 27	83	75.997	0.916	0.000~18.612/18.612
LG 28	26	73.516	2.828	8.942~24.714/15.772
LG 29	90	70.097	0.779	5.690~11.425/5.735
LG 30	21	67.415	3.210	5.834~34.453/28.619
LG 31	33	65.647	1.989	45.331~62.997/17.666
LG 32	102	65.061	0.638	0.000~7.486/7.486
LG 33	78	63.218	0.810	42.926~63.218/20.292
LG 34	36	58.634	1.629	31.041~42.810/11.769
LG 35	36	57.235	1.590	17.074~29.374/12.300
LG 36	102	56.731	0.556	6.994~11.226/4.232
LG 37	99	55.137	0.557	37.494~44.753/7.259
LG 38	15	47.958	3.197	15.331~33.490/18.159
LG 39	21	45.096	2.147	0.024~15.935/5.911
LG 40	73	42.609	0.584	17.880~23.721/5.840
LG 41	60	40.998	0.683	0.000~8.253/8.253
LG 42	29	40.073	1.382	0.000~24.843/24.843
LG 43	75	29.455	0.393	22.323~26.794/4.471
LG 44	41	25.477	0.621	20.197~25.477/5.280
LG 45	22	21.530	0.979	2.770~11.625/8.855
LG 46	26	17.737	0.682	6.316~13.591/7.275
LG 47	26	15.564	0.599	8.531~15.564/7.033
LG 48	15	14.612	0.974	4.273~13.932/9.659
Total	3567	4161.555	1.167	LG10 (0.682~30.146/29.464)

were searched in the Pacific white shrimp genome database (GenBank no. QCYY00000000.1), and the aligned shrimp genome scaffolds were identified. The genes contained in the genome scaffolds (called the scaffold genes) were obtained, and the stress- and growth-related scaffold genes were annotated and summarized according to previous studies.

All the stress-related scaffold genes were compared with the high-pH transcriptome data from our previous work (S7 Table in Huang et al. 2018), and the coexisting candidate genes for high-pH response were discovered. To verify the mRNA expression patterns of the candidate high-pH response genes, healthy cultured shrimp (supplied by Yuehai Feed Group Co., LTD, Zhanjiang, China; average weight, 11.09 ± 2.37 g) were selected, and the three shrimp groups were treated in pH 8.0 seawater (control pH), pH 9.0 seawater, and pH 9.3 seawater. The high-pH values of the seawater were maintained as described previously (Wang et al. 2009; Huang et al. 2018). Total RNA was extracted from the posttreated gill tissues of the shrimp at 0, 1, 6, 12, 24, and 48 h. Real-time PCR analysis was carried out using the primers listed in Supplementary Table 1. The relative expression levels of the candidate genes were obtained according to the $2^{-\Delta\Delta CT}$ method by normalizing to the expression of the *L. vannamei* β-actin gene (Livak and Schmittgen 2001).

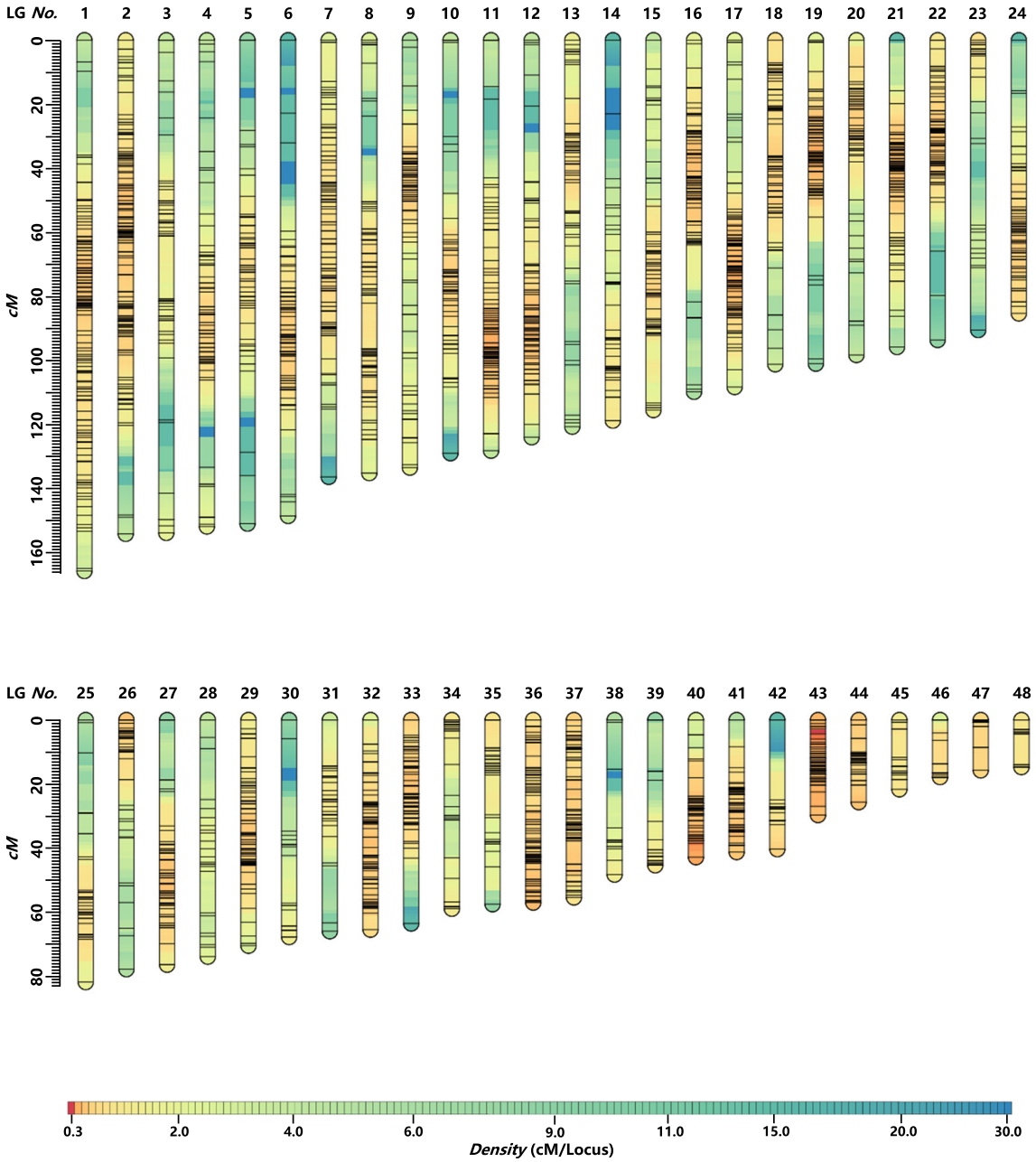

Fig. 2 Linkage group lengths and marker distributions of a high-resolution genetic map of *L. vannamei*. cM: centimorgan. LG: linkage group

Table 2 High-pH trait-related and growth trait-related QTLs in *L. vannamei*

Trait	QTL	LG	Location (cM)	Interval length (cM)	QTL peak position (cM)	Peak LOD	Peak expl. (%)
BW	BW-1	1	101.750~102.050	0.300	102.050	2.56	9.0
	BW-2	1	121.889~122.822	0.933	121.889	2.92	10.3
HP	HP-1	4	64.170~67.590	3.420	67.250	2.75	8.3
	HP-2	4	69.847~70.350	0.503	70.350	2.68	9.8
	HP-3	4	144.486~149.146	4.660	149.146	3.47	65.2
	HP-4	13	18.249~25.249	7.000	25.249	2.97	14.6
	HP-5	13	29.092~29.770	0.678	29.170	2.59	8.0
	HP-6	13	33.057~33.153	0.096	33.119	2.74	8.2
	HP-7	13	35.098~37.845	2.747	36.472	2.59	9.4
	HP-8	18	36.201~37.345	1.144	37.345	2.61	7.9
	HP-9	18	40.218~42.158	1.940	40.850	2.61	8.4
	HP-10	26	35.183~44.609	9.426	36.609	2.89	13.8
	HP-11	26	71.023~77.023	6.000	74.023	2.70	63.4
	HP-12	36	49.451~51.492	2.041	50.805	2.74	9.0

Results

Summary of the Data

The high-pH challenge data were analyzed. In total, 21 shrimps (survival rate of 60.0%) survived after treatment in the high-pH environment of 9.1 for 48 h, 3 (survival rate of 8.6%) survived after treatment in the high-pH environment of 9.3 for 48 h, and all died after treatment in a high-pH environment of 9.5 for 12 h (Fig. 1a).

The high-pH value of 9.3 was set as the stress environment, and 148 progenies were treated in pH 9.3 seawater; with the ability or inability of the shrimp to resist a high-pH environment, 9 different stages were determined (Fig. 1b). Nine individuals (6.08%) died in the first stage (0–2 h), and 11 (7.43%) progenies survived beyond 48 h of treatment (Fig. 1b). The body weights were immediately obtained when the shrimp were dying under the pH 9.3 stress condition; the minimum shrimp body weight was 0.048 g, the maximum shrimp body weight was 1.100 g, the mean body weight was 0.319 ± 0.211 g, and the body weight values of the shrimp individuals were continuous (Fig. 1c).

Sequencing and Genotyping

A total of 150 ddRAD libraries were constructed from the two parents and their 148 offspring. The mean value of the GC% in the offspring was 43.67 ± 0.73% (Supplementary Table 2). The adenine bases (A) nearly overlapped the thymine bases (T), and the guanine bases (G) nearly overlapped the cytosine bases (C) (Fig. 1d, Supplementary Table 2). After filtering, the female parent had 2.17 Gb of clean data (GC rate of 42.16% and a Q30 rate of 90.08%), and the male parent had 2.58 Gb of clean data (GC rate of 43.21% and Q30 rate of 90.18%). The clean reads of the progenies ranged from 5.42 to 27.97 million, and the clean reads of the offspring ranged from 0.80 to 4.07 Gb (average GC rate of 43.61 ± 0.73 and mean Q30 value of 89.54 ± 1.12) (Supplementary Table 3). All clean data were deposited into the US National Center for Biotechnology Information (NCBI) Sequence Read Archive (SRA, http://www.ncbi.nlm.nih.gov/Traces/sra) under GenBank accession no. PRJNA532795. A total of 10,465 markers were detected from more than 90% of the progenies (Fig. 1e), and after a Mendelian fit test ($P \geq 0.05$), 3894 high-quality markers (three types of markers including 2446 "lm × ll" markers, 1308 "nn × np" markers, and 140 hk × hk markers) were used to construct the consensus genetic map (Fig. 1e).

Construction of Linkage Maps

A ddRAD-based linkage map of *L. vannamei* was constructed with high-quality markers. The LGs containing fewer than 15 markers were discarded, and the final integrated map consisted of 48 LGs, including 3567 high-quality segregating SNP markers (327 high-quality markers were discarded or not located) (Table 1, Fig. 2). The total map length was 4161.555 cM, the average interlocus length was 1.167 cM, the genetic length of the LGs ranged from 14.612 cM (LG48) to 165.922 cM (LG 1), and the average interval length of the LGs ranged from 0.393 cM (LG 43) to 3.210 cM (LG 30) (Table 1, Fig. 2). Detailed information, including the marker names, tag sequences, and positions of the LGs, is provided in Supplementary Tables 4–5.

QTL Analysis of High-pH Tolerance and Growth Traits

For the HP trait, 12 QTLs were discovered (LOD value > 2.5) (Table 2) and were distributed in 5 different LGs (LG 4, LG

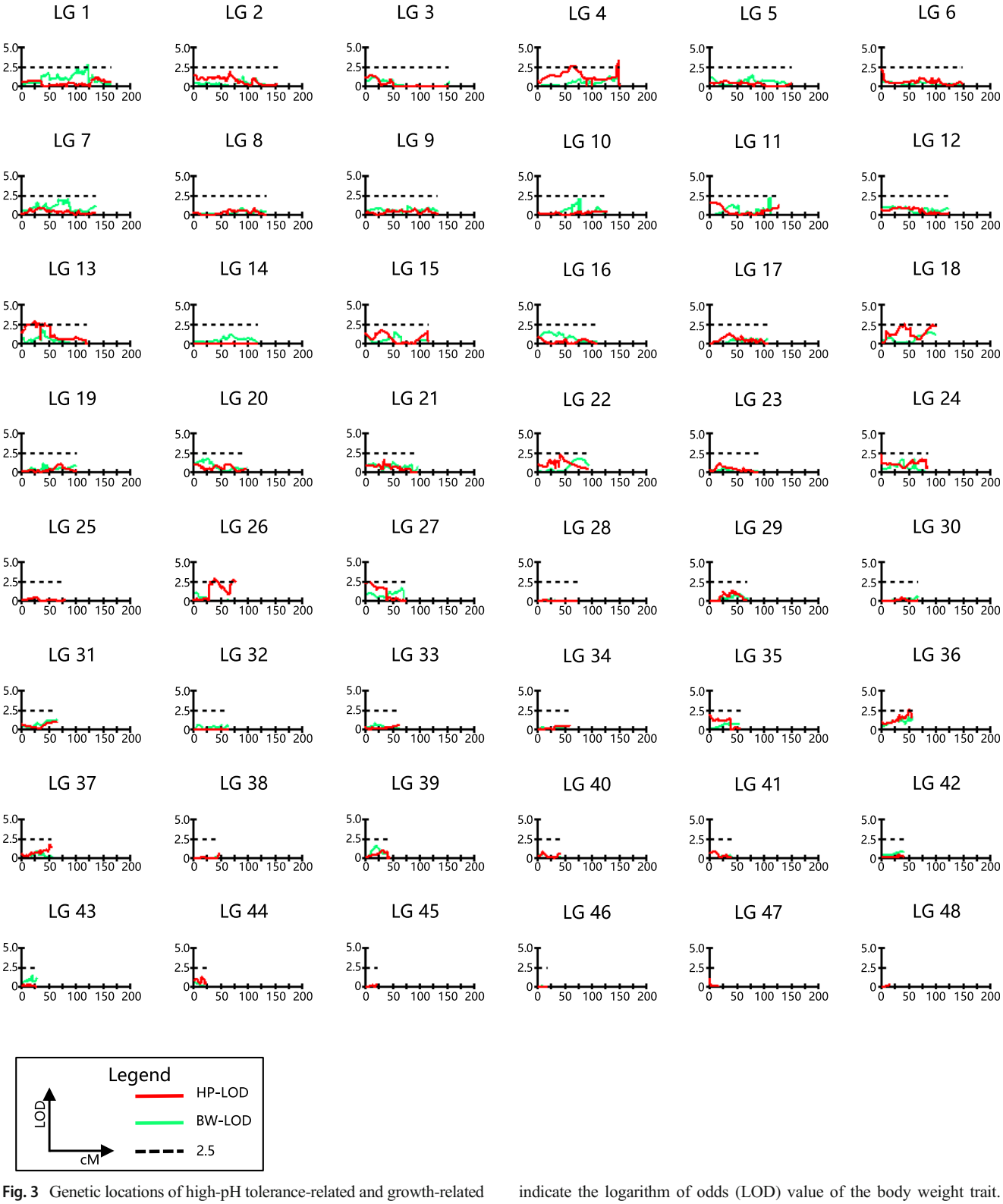

Fig. 3 Genetic locations of high-pH tolerance-related and growth-related (body weight) QTLs on 48 LGs of *L. vannamei*. The red lines indicate the logarithm of odds (LOD) value of the high-pH trait. The green lines indicate the logarithm of odds (LOD) value of the body weight trait. The dashed lines indicate a cutting threshold of LOD at 2.5

13, LG 18, LG 26, and LG 36) (Figs. 3 and 4). The most prominent QTL was HP-3, with an LOD value of 3.47; this QTL was 4.660 cM in length and explained 65.2% of the phenotypic variation. The detailed QTL information for the HP trait is available in Supplementary Table 4.

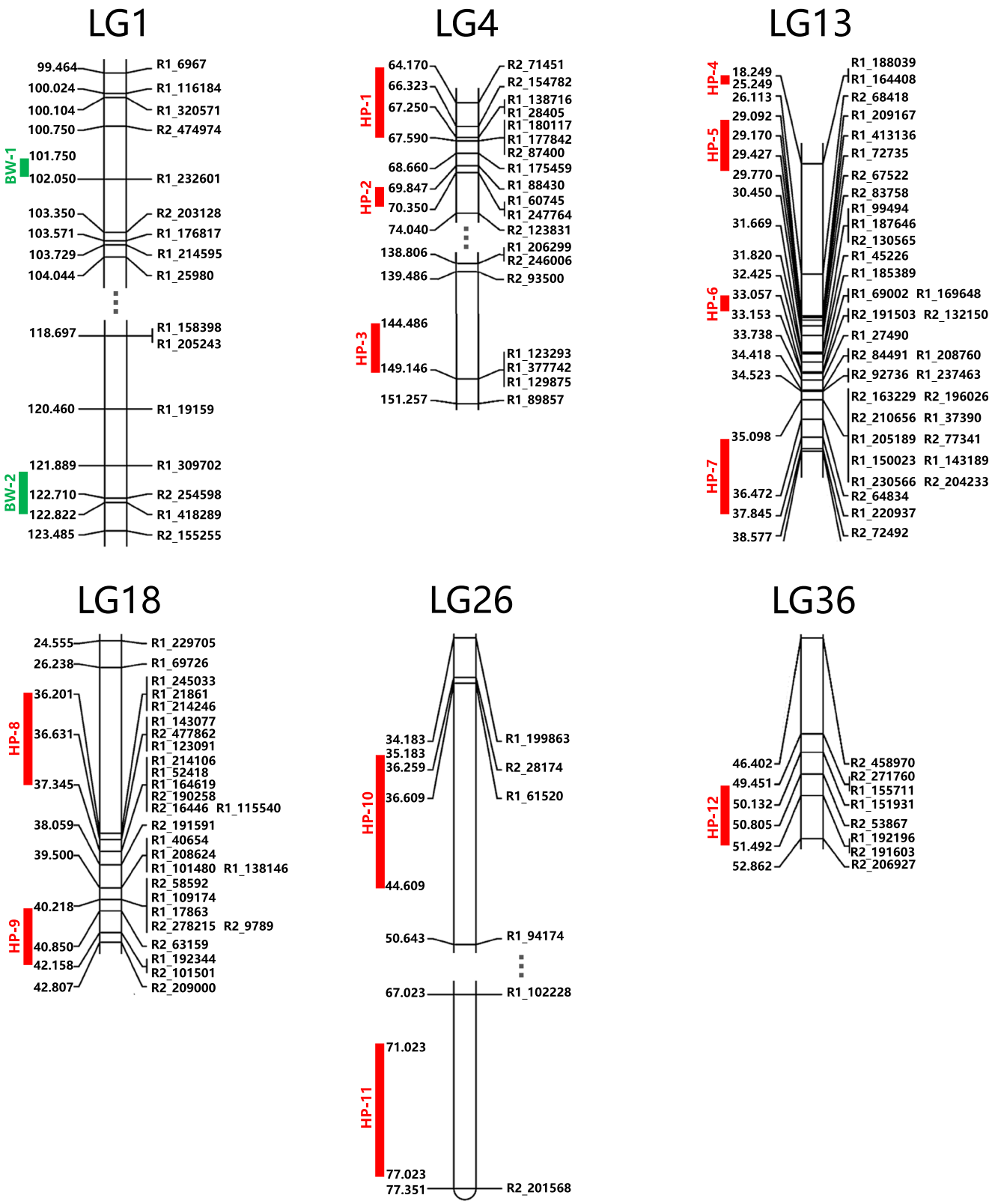

Fig. 4 Distribution of the high-pH tolerance-related and growth-related (body weight) QTLs on 6 different linkage groups. The value of the genetic distance (centimorgan, cM) was displayed on the left side of the LGs, and the related markers are presented on the right side of the LGs

For the BW trait, 2 QTLs were detected (LOD value > 2.50) (Table 2), and the BW QTLs were located in LG 1 (Figs. 3 and 4). BW-2 was the major QTL (interval length of 0.933 cM), and it had an LOD value of 2.92 and explained

Table 3 Summary of the aligned *L. vannamei* scaffolds

QTL	Location (LG_cM)	Related marker (LOD)	Aligned *L. vannamei* scaffold	Aligned position (bp)
HP-1	4_64.170	R2_71451 (2.62)	LVANscaffold_1261	408,520–408,667
	4_66.323	R2_154782 (2.64)	LVANscaffold_2170	136,117–136,266
	4_67.250	R1_138716 (2.75)	LVANscaffold_2513	508,647–508,790
		R1_28405 (2.73)	LVANscaffold_1261	390,463–390,606
	4_67.590	R1_180117 (2.54)	None	None
		R1_177842 (2.54)	None	None
		R2_87400 (2.54)	LVANscaffold_2723	345,175–345,323
HP-2	4_69.847	R1_88430 (2.44)	LVANscaffold_3340	1,702,538–1,702,681
	4_70.350	R1_60745 (2.68)	LVANscaffold_2027	1,829,105–1,829,248
		R1_247764 (2.33)	LVANscaffold_2027	1,823,768–1,823,914
HP-3	4_139.486	R2_93500 (1.08)	LVANscaffold_2067	164,203–164,054
	4_149.146	R1_123293 (3.47)	LVANscaffold_1243	66,155–66,298
		R1_377742 (0.35)	LVANscaffold_2120	126,607–126,750
		R1_129875 (0.35)	LVANscaffold_1243	24,820–24,963
HP-4	13_18.249	R1_188039 (2.34)	LVANscaffold_2654	432,603–432,747
		R1_164408 (2.57)	LVANscaffold_2664	379,562–379,705
	13_25.249	R2_68418 (1.95)	None	None
HP-5	13_29.092	R1_209167 (2.56)	LVANscaffold_2881	408,553–408,696
	13_29.170	R1_413136 (2.59)	LVANscaffold_2881	251,318–251,465
	13_29.427	R1_72735 (2.53)	LVANscaffold_1662	42,883–43,026
	13_29.770	R2_67522 (2.57)	LVANscaffold_2421	329,038–329,187
HP-6	13_33.057	R1_69002 (2.63)	LVANscaffold_1586	61,779–61,922
		R1_169648 (2.74)	LVANscaffold_2667	644,642–644,746
	13_33.153	R2_191503 (2.73)	LVANscaffold_1662	43,043–43,190
		R2_132150 (2.73)	LVANscaffold_2881	370,831–370,977
HP-7	13_35.098	R2_163229 (2.33)	LVANscaffold_1348	520,816–520,965
		R2_196026 (2.33)	LVANscaffold_1348	535,763–535,912
		R2_210656 (2.33)	LVANscaffold_3491	207,354–207,503
		R1_37390 (2.33)	LVANscaffold_2256	136,990–137,133
		R1_205189 (2.29)	LVANscaffold_2256	23,448–23,591
		R2_77341 (0.41)	LVANscaffold_3491	201,935–202,081
		R1_150023 (0.41)	LVANscaffold_218	238,219–238,363
		R1_143189 (2.57)	LVANscaffold_720	254,204–254,347
		R1_230566 (2.50)	LVANscaffold_1348	521,297–521,154
		R2_204233 (2.50)	LVANscaffold_3491	159,181–159,327
	13_36.472	R2_64834 (2.59)	LVANscaffold_667	124,209–124,358
	13_37.845	R1_220937 (2.58)	LVANscaffold_2974	331,144–331,285
HP-8	18_36.201	R1_245033 (2.53)	None	None
		R1_21861 (2.54)	LVANscaffold_1059	337,995–338,138
		R1_214246 (2.54)	None	None
	18_36.631	R1_143077 (2.59)	LVANscaffold_697	486,909–487,052
		R2_477862 (2.59)	LVANscaffold_697	499,284–499,431
		R1_123091 (2.59)	LVANscaffold_1695	112,979–113,122
	18_37.345	R1_214106 (2.61)	LVANscaffold_2698	1,229,635–1,229,778
		R1_52418 (2.60)	LVANscaffold_2698	1,176,194–1,176,337
		R1_164619 (2.46)	LVANscaffold_2804	88,042–88,184
		R2_190258 (2.51)	LVANscaffold_2698	729,316–729,465
		R2_16446 (2.51)	LVANscaffold_308	212,359–212,508
		R1_115540 (2.51)	LVANscaffold_813	429,472–429,615

Table 3 (continued)

QTL	Location (LG_cM)	Related marker (LOD)	Aligned *L. vannamei* scaffold	Aligned position (bp)
HP-9	18_40.218	R2_58592 (2.55)	None	None
		R1_109174 (2.55)	LVANscaffold_308	41,192–41,335
		R1_17863 (2.55)	LVANscaffold_21	64,205–64,335
		R2_278215 (2.55)	LVANscaffold_697	644,667–644,816
		R2_9789 (2.55)	LVANscaffold_2804	90,726–90,873
	18_40.850	R2_63159 (2.61)	LVANscaffold_813	429,255–429,404
	18_42.158	R1_192344 (2.51)	LVANscaffold_813	272,801–272,944
		R2_101501 (2.51)	LVANscaffold_25	33,276–33,425
HP-10	26_34.183	R1_199863 (2.19)	LVANscaffold_1634	144,966–145,109
	26_36.259	R2_28174 (2.89)	LVANscaffold_4282	376,987–377,136
	26_36.609	R1_61520 (2.89)	LVANscaffold_2885	283,535–283,668
	26_50.643	R1_94174 (1.63)	LVANscaffold_969	301,389–301,529
HP-11	26_67.023	R1_102228 (1.26)	LVANscaffold_1314	600,972–601,115
	26_77.351	R2_201568 (2.46)	None	None
HP-12	36_49.451	R2_271760 (1.87)	None	None
		R1_155711 (2.54)	LVANscaffold_1676	329,326–329,469
	36_50.132	R1_151931 (2.65)	LVANscaffold_2468	96,946–97,089
	36_50.805	R2_53867 (2.74)	LVANscaffold_2215	669,156–669,305
	36_51.492	R1_192196 (2.73)	LVANscaffold_3606	50,006–50,133
		R2_191603 (2.50)	None	None
BW-1	1_102.050	R1_232601 (2.56)	LVANscaffold_193	6893–7036
BW-2	1_121.889	R1_309702 (2.92)	LVANscaffold_4257	116,374–116,516
	1_122.710	R2_254598 (2.73)	LVANscaffold_589	263,658–263,807
	1_122.822	R1_418289 (2.53)	LVANscaffold_1229	677,175–677,318

10.3% of the phenotypic variation (Table 2). The major BW-related genes might be located between the SNP markers of R1_309702 and R1_418289. Another BW QTL is listed in Table 2 and Fig. 4, and the detailed QTL information for the BW trait is provided in Supplementary Table 5.

Identification of the High-pH Response Gene Candidates

In total 73 HP and BW QTL markers were aligned to 46 *L. vannamei* scaffolds (Table 3). In the HP-2 QTL, the marker "R1_60745," with an LOD value of 2.68 in LG4, was aligned to the *L. vannamei* scaffold "LVANscaffold_2027," and the marker "R1_247764" in this QTL was aligned to the same *L. vannamei* scaffold, indicating a close genetic distance between the two markers (Table 3).

The stress-related genes contained in these *L. vannamei* scaffolds were summarized according to previous studies (Table 4). The expression levels of the stress-related genes were investigated using high-pH transcriptome data from our previous work (Huang et al. 2018), and six candidate high-pH response genes were discovered: hypoxia inducible factor 1 beta (HIF1b), transcription initiation factor TFIID subunit 3 (TAF3), glutamyl aminopeptidase (ENPEP), discoidin domain-containing receptor 2-like (DDR2), phosphatidylcholine: ceramide cholinephosphotransferase 1-like (SGMS1) and histone H2A.V-like (H2AFV) (Table 4). With the same method, 5 growth-related genes were obtained (Table 5).

To further verify the results in this study, real-time PCR was carried out to identify the expression patterns of the high-pH response genes. The expression levels of the 6 candidate genes were significantly influenced by the high-pH treatment, and 5 (all except the ENPEP gene) of the 6 candidate genes were consistent with the high-pH transcriptome data (Fig. 5). Specifically, the HIF1b and SGMS1 genes were significantly upregulated for 6 h in the high-pH environment, and TAF3 and DDR2 were obviously downregulated in the first 6 h in response to the high-pH stress. The H2AFV gene was downregulated in the first few hours but was then substantially upregulated in the following hours in response to high-pH stress, and the results validate the candidate high-pH response genes (Fig. 5).

Discussion

Full-sib families provide basic materials for genetic breeding programs in aquatic species, and they are particularly

Table 4 The candidate high-pH response genes in *L. vannamei* scaffolds

Located marker (LOD)	Scaffold[a]	Stress genes in LVANscaffold	GeneID[b]	CT[c]	T_1[d]	T_48[e]	Gene description
R1_143077 (2.59); R2_477862 (2.59); R2_278215 (2.55)	LVANscaffold_697	Hypoxia inducible factor 1 beta (GenBank: ROT83372.1)	Unigene36136_All	0.13/328.96	20.76/1059.02	0.01/340.01	Respond to anti-tumor effects under hypoxic conditions (Soñanez-Organis et al. 2009, Choi et al. 2014)
		Transcription initiation factor TFIID subunit 3 (GenBank: ROT83365.1)	CL12063.Contig2_All	1.43/328.96	0.12/1059.02	0.85/340.01	Plays a central role in mediating promoter responses to various activators and repressors (Malkowska et al. 2013)
		Ubiquitin-conjugating enzyme E2 S (GenBank: ROT83376.1)	None	None	None	None	Contribute to cellular stress-tolerance mechanisms (Chuang and Madura 2005)
		YTH domain family protein 1 (GenBank: ROT83367.1; ROT83366.1)	None	None	None	None	Promotes mRNA translation efficiency (Dai et al. 2018)
		SOSS complex subunit B1-A-like (GenBank: ROT83363.1)	None	None	None	None	Associates with DNA lesions and influences diverse endpoints in the cellular DNA damage (Kang et al. 2006)
		Putative serine/threonine-protein kinase (GenBank: ROT83358.1)	None	None	None	None	Play a role in the regulation of cell proliferation, programmed cell death (apoptosis), cell differentiation, and embryonic development (Cross et al. 2000)
R1_209167 (2.56); R1_413136 (2.59); R2_132150 (2.73)	LVANscaffold_2881	Glutamyl aminopeptidase (GenBank: ROT66889.1)	CL12393.Contig1_All	1.67/328.96	1.36/1059.02	7.03/340.01	Help to regulate blood pressure (Goto et al. 2006)
		Phosphoinositide 3-kinase isoform a (GenBank: ROT66890.1)	None	None	None	None	Key cascade downstream of several protein kinases (Toulany and Rodemann 2015)
		Indole-3-acetaldehyde oxidase-like (GenBank: ROT66898.1)	None	None	None	None	Responses to various environmental stresses in plant seed (Seo et al. 2000)
		Double-strand break repair protein MRE11A (GenBank: ROT66880.1)	None	None	None	None	Plays a central role in double-strand break repair, DNA recombination (Carney et al. 1998)
		Ubiquitin-conjugating enzyme E2 G1 (GenBank: ROT66879.1)	None	None	None	None	Degrading substrates tagged by polyubiquitin chains (Van Wijk and Timmers 2010)
R1_214106 (2.61); R1_52418 (2.60); R2_190258 (2.51)	LVANscaffold_2698	Discoidin domain-containing receptor 2-like (GenBank: ROT68288.1)	CL5031.Contig4_All	1.25/328.96	0.16/1059.02	2.52/340.01	Have a role in wound healing (Márquez and Olaso 2014)
		Phosphatidylcholine: ceramide cholinephosphotransferase 1-like (GenBank: QCYY01002696.1)	Unigene4495_All	2.08/328.96	15.86/1059.02	2.15/340.01	Associated with suppressed ceramide response and apoptotic resistance after photodamage (Separovic et al. 2007)
		Coiled-coil domain-containing protein 50 (GenBank: ROT68284.1)	None	None	None	None	Have effects on cell survival (Blagoev et al. 2004)
R2_210656 (2.33); R2_77341 (0.41); R2_204233 (2.50)	LVANscaffold_3491	Histone H2A.V-like (GenBank: ROT63113.1)	CL12379.Contig2_All	6.34/328.96	0.01/1059.02	6.23/340.01	Transcription regulation, DNA repair, DNA replication, and chromosomal stability (Van Daal and Elgin 1992)
		Oxysterol-binding protein 1A (GenBank: ROT63114.1)	None	None	None	None	Controls a key signaling pathway in the cell (Wang 2005)
R2_163229 (2.33); R2_196026 (2.33); R1_230566 (2.50)	LVANscaffold_1348	Breast cancer type 1 susceptibility protein-like (GenBank: ROT78680.1)	None	None	None	None	DNA damage repair, cell growth, and apoptosis (Deng and Brodie 2000)
		COP9 signalosome complex subunit 2-like (GenBank: ROT78673.1)	None	None	None	None	DNA damage (Groisman et al. 2003)

Table 4 (continued)

Located marker (LOD)	Scaffold[a]	Stress genes in LVANscaffold	GeneID[b]	CT[c]	T_1[d]	T_48[e]	Gene description
R1_115540 (2.51); R2_63159 (2.61); R1_192344 (2.51)	LVANscaffold_813	E3 ubiquitin-protein ligase UBR7 (GenBank: ROT82507.1)	None	None	None	None	Ubiquitination and degradation (Zimmerman et al. 2014)
		Transcription elongation factor S-II-like (GenBank: ROT82506.1)	None	None	None	None	Critical for efficient release of Pol II from the hsp70 promoter region upon heat induction (Adelman et al. 2005)
		Phosphoinositide 3-kinase adapter protein 1 (GenBank: ROT82513.1)	None	None	None	None	Impaired immune function and increased susceptibility to apoptosis (MacFarlane et al. 2008)

The values were expressed as fragments per kilobase of transcript per million mapped reads (FPKM) in the transcriptome data

[a] The aligned accession number of *L. vannamei* scaffold by the HP-QTL markers

[b] The GeneID in the high-pH transcriptome data of our previous study (Huang et al. 2018)

[c] The expression ratio with the β-actin (β-actin of *L. vannamei*, GeneID: CL1300.Contig14_All) in the control group (CT) of the transcriptome data

[d] The expression ratio with the β-actin (β-actin of *L. vannamei*, GeneID: CL1300.Contig14_All) in the high-pH 1 h group (T_1) of the transcriptome data

[e] The expression ratio with the β-actin (β-actin of *L. vannamei*, GeneID: CL1300.Contig14_All) in the high-pH 48 h group (T_48) of the transcriptome data

important for mapping trait-related QTLs based on RAD-Seq technologies. For example, F1 full-sib families (including the two parents) have been generated and used to build ddRAD libraries in several aquatic species, such as *Oreochromis niloticus* (Li et al. 2017), *Trachinotus blochii* (Zhang et al. 2018), and *Larimichthys crocea* (Kong et al. 2019). Generally, the F1 full-sib families were constructed with methods of directional crossing (a pair of parents for mating) (Fu et al. 2016; Li et al. 2017; Kong et al. 2019) or undirectional crossing (several or more pairs of parents for mating) (Shao et al. 2015). According to the propagation characteristic of the shrimp *L. vannamei*, mating a pair of fertile shrimp is difficult to achieve in nature. Yu et al. (2015, 2019) used the "undirectional cross" method to create four combined full-sib *L. vannamei* families and then used 10 microsatellite loci to select the mapping family; an F1 full-sib family of 205 progenies was constructed, and their parental genomic DNA was identified (Alcivar-Warren et al. 2007; Yu et al. 2015; Yu et al. 2019). In the present study, the "semidirectional cross" method was used to generate the *L. vannamei* F1 full-sib family, with 148 progenies and 2 parental individuals (not just the parental genomic DNA) of the mapping family being visually identified. This method may be a quick way to generate full-sib families, which would be beneficial for genetic research on the shrimp *L. vannamei*.

SNP markers are ideal for the construction of genetic linkage maps (Bourgeois et al. 2013; Stölting et al. 2013; Wang et al. 2013a, 2013b; Zhang et al. 2018). SNPs are the most common type of DNA polymorphism in the genome, have a low mutation rate and high genetic stability, and are amenable to high-throughput genotyping (Berthier-Schaad et al. 2007; Shao et al. 2015; Zhang et al. 2018; Kong et al. 2019). In total, 3567 high-quality SNP markers were constructed for the linkage map in the present work. The number of SNPs identified was less than that identified in the previous study on *L. vannamei* by Yu et al. (2015) (6359 SNPs were selected for mapping) but more than that identified in the study on *Hypophthalmichthys nobilis* by Fu et al. (2016) (3121 SNPs were used for mapping). Genetic linkage maps constructed by SNP markers are important resources for various genetic studies, including comparative genomics, functional gene mapping, candidate gene positional cloning, and genome assembly (Yue 2014; Xu et al. 2014; Kujur et al. 2015; Zhang et al. 2018; Kong et al. 2019). In total, 48 LGs with a total map length of 4161.555 cM and an average interlocus length of 1.167 cM were obtained in the present study. The number of LGs was close to those obtained in previous studies; examples include 44 pseudochromosomes (Zhang et al. 2019), 44 sex-averaged LGs (Yu et al. 2015), and 45 sex-averaged LGs (Du et al. 2010). Our results might be useful for future genomic assembly research on the shrimp *L. vannamei*.

With the help of a high-resolution genetic map, fine mapping of QTLs is an efficient approach for identifying genetic

Table 5 The candidate growth-related genes in *L. vannamei* scaffolds

Located marker (LOD)	QTL	Scaffold[a]	Protein number	Growth-related gene	Gene description
R1_232601 (2.56)	BW-1	LVANscaffold_193	5	Putative ATP-dependent RNA helicase DDX43 (GenBank: ROT85772.1)	Required for tumor growth through promoting RAS protein expression (Linley et al. 2012)
R1_309702 (2.92)	BW-2	LVANscaffold_4257	0	None	None
R2_254598 (2.73)	BW-2	LVANscaffold_589	2	None	None
R1_418289 (2.53)	BW-2	LVANscaffold_1229	15	ATP-binding cassette transporter sub-family B member 8 (ROT79549.1)	Related to the activity of cytosolic (Ichikawa et al. 2012)
				Triacylglycerol lipase (ROT79548.1, ROT79547.1, ROT79544.1)	Important energy substrate at rest and during physical activity (Watt and Spriet 2010)
				Putative lipase 3-like (ROT79545.1)	Have key roles in insect lipid acquisition, storage, and mobilization (Horne et al. 2009)
				Insulin receptor substrate 2-B, partial (ROT79542.1)	Can prevent obesity and diabetes in mice (Lin et al. 2004)

[a] The aligned accession no. of *L. vannamei* scaffold by the BW QTL markers

loci and the candidate genes underlying these quantitative traits of interest (Shao et al. 2015; Wang et al. 2018). Growth is a priority trait for genetic improvement, and mapping of growth-related QTLs has been widely performed in studies on various aquatic species (Andriantahina et al. 2013, Yue 2014, Tong and Sun 2015, Wang et al. 2018). In the present work, 2 growth-related (body weight) QTLs were detected, both of which were located in LG1 of the genetic map. Several growth-related QTL studies have been previously performed on *L. vannamei*. For example, Andriantahina et al. (2013) used amplified fragment length polymorphism (AFLP) and simple sequence repeat (SSR) markers to

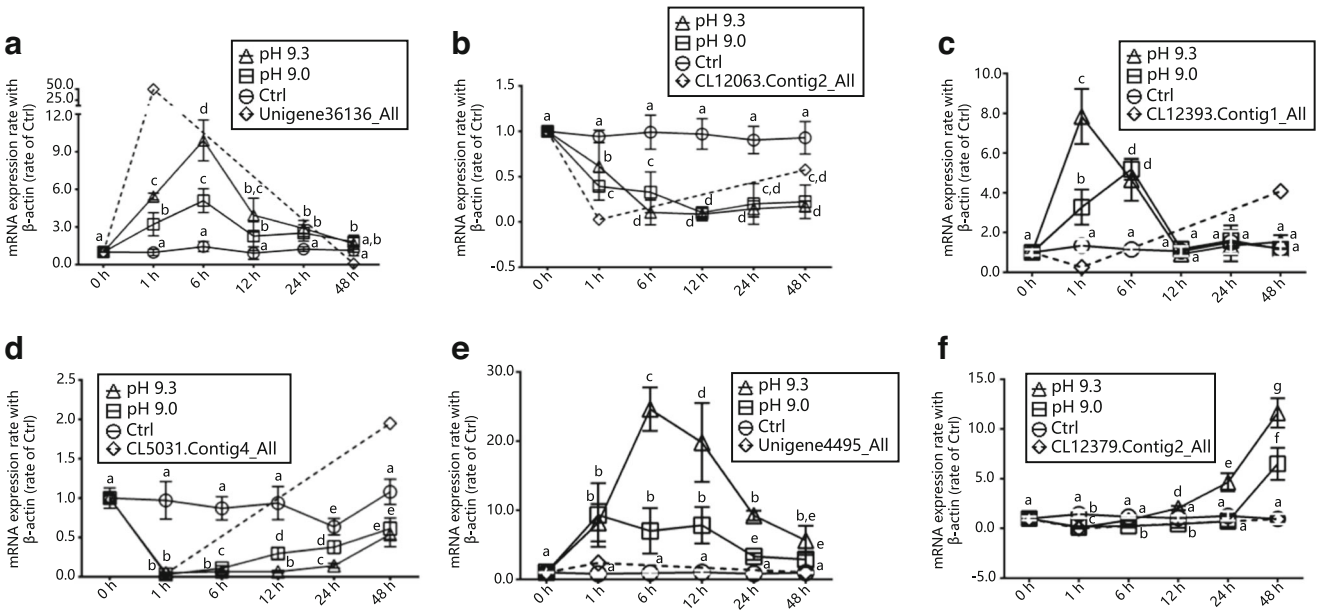

Fig. 5 Transcriptional expression of the candidate high-pH response genes. **a** Expression pattern of the gene "hypoxia inducible factor 1 beta (HIF1b)". **b** Expression pattern of the gene "transcription initiation factor TFIID subunit 3 (TAF3)". **c** Expression pattern of the gene "glutamyl aminopeptidase (ENPEP)". **d** Expression pattern of the gene "discoidin domain-containing receptor 2-like (DDR2)". **e** Expression pattern of the gene "phosphatidylcholine: ceramide cholinephosphotransferase 1-like (SGMS1)". **f** Expression pattern of the gene "histone H2A.V-like (H2AFV)". Gill tissues of *L. vannamei* treated in high-pH environment for 0, 1, 6, 12, 24, and 48 h. The data are presented as the mean ± SE (n = 6), and the groups denoted by the same letter exhibit a similar expression levels ($P > 0.05$, two-way ANOVA followed by Fisher's LSD test). Dotted lines indicate the expression pattern of the high-pH transcriptome data (the shrimp were treated in the pH 9.3 environment for 1 and 48 h) from our previous work (Huang et al. 2018)

construct a genetic map, and 14 growth-related QTLs were identified (Andriantahina et al. 2013). Yu et al. (2015) detected several QTLs for body weight and body length based on a high-density linkage map (Yu et al. 2015); however, candidate gene associations with the growth trait were not identified due to limited genomic information (Yu et al. 2019). In the present study, 2 growth-related QTLs were detected in 55-day-old shrimp using *L. vannamei* genomic scaffolds (Zhang et al. 2019), and 5 growth-related candidate genes were detected and demonstrated to be associated with cell growth or energy metabolism. The gene "putative ATP-dependent RNA helicase DDX43" of BW-1 in this paper is thought to be required for tumor growth through the promotion of RAS protein expression (Linley et al. 2012). The Ras-related protein Rap-2a was identified as being significantly associated with the growth trait by applying GWAS in two independent populations of *L. vannamei* (Yu et al. 2019) and was discovered to be associated with head size regulation in catfish (*Ictalurus punctatus*) (Geng et al. 2016). The detection of the 5 candidate genes in this study might be relevant to the growth trait, the Ras-related proteins might be associated with the growth trait of *L. vannamei* at 55 days of age, and the location of the 2 growth-related QTLs (BW-1 and BW-2) in this study might be valid.

The balance of acidic-alkaline ions in water is important for aquatic crustaceans (Fehsenfeld et al. 2011; Roggatz et al. 2016; de Vries et al. 2016; Wu et al. 2017; Huang et al. 2018). The farming of *L. vannamei* in high-pH environments might affect the final production (Huang et al. 2018), and the high-pH tolerance of shrimp has become an important trait in the culturing industry in saline-alkali water areas. In the present study, the first genetic study on the high-pH tolerance trait for *L. vannamei*, 12 high-pH tolerance QTLs were discovered. With the development of genomic research on *L. vannamei* (Zhang et al. 2019), tag sequences of the SNP markers are now available that align with the genomic scaffolds of the shrimp; in the present study, 21 stress-related genes were summarized according to the annotation of the scaffold genes. Our previous work revealed the molecular basis of response to high-pH stress by analyzing *L. vannamei* transcriptome data (Huang et al. 2018); and we identified 6 candidate high-pH response genes based on RNA- and RAD-Seq results. The expression patterns of the 6 candidate genes were demonstrated to be significantly influenced by the high-pH environment, with 5 of the 6 candidate high-pH response genes showing results consistent with those of the RNA-Seq, indicating the important roles of those genes in response to high-pH stress and validating the locations of the HP QTLs for *L. vannamei* in this study.

In conclusion, a "semidirectional cross" method was used to generate the *L. vannamei* full-sib family in the present study. High-pH tolerance and growth trait-related QTLs were detected in one genetic map by ddRAD-Seq, and candidate genes associated with the high-pH tolerance and growth traits were discovered by alignment them with the *L. vannamei* genomic scaffolds and analysis of high-pH transcriptome data. We herein provide baseline data and the first report of shrimp breeding to induce high-pH tolerance traits. Our results will be beneficial for further MAS work and might be useful for promoting genomic research on the shrimp *L. vannamei*.

Acknowledgments We thank the anonymous reviewers for comments on the manuscript.

Authors' Contributions WH and CH contributed to project conception. Experiment and data analysis was conducted by WH, CC, JL, XZ, CR, XJ, TC, KC, and HL. The manuscript was prepared by WH. All authors read and approved the final manuscript.

Funding Information This work was supported by the National Natural Science Foundation of China (No. 31602135), Institution of South China Sea Ecology and Environmental Engineering, Chinese Academy of Sciences (No. ISEE2018PY03), the Science & Technology Promoting Projects for Oceanic & Fishery in Guangdong Province (SDYY-2018-01), and the Guangdong Province Program (2017B030314052, 2018A030313857, 2016A030310112, 2015A030310120, 2015B020231007 and A2015230).

Compliance with Ethical Standards

Statement of Human and Animal Rights Shrimp care and experiments were carried out according to the Care and Use of Agricultural Animals in Agricultural Research and Teaching and approved by the Science and Technology Bureau of China. Approval from the Department of Wildlife Administration was not required for the experiments conducted in this paper. All experiments in this paper were performed with permits obtained from the Government of the People's Republic of China and endorsed by the Animal Experimentation Ethics Committee of Chinese Academy of Sciences.

Conflict of Interest The authors declare that they have no competing interests.

References

Abdelrahman ElHady M, Alcivar-Warren A, Allen S, Al-Tobasei R, Bao L, Beck B, Blackburn H, Bosworth B, Buchanan J, Chappell J, Daniels W, Dong S, Dunham R, Durland E, Elaswad A, Gomez-Chiarri M, Gosh K, Guo X, Hackett P, Hanson T, Hedgecock D, Howard T, Holland L, Jackson M, Jin Y, Khalil K, Kocher T, Leeds T, Li N, Lindsey L, Liu S, Liu Z, Martin K, Novriadi R, Odin R, Palti Y, Peatman E, Proestou D, Qin G, Reading B, Rexroad C, Roberts S, Salem M, Severin A, Shi H, Shoemaker C, Stiles S, Tan S, Tang KF, Thongda W, Tiersch T, Tomasso J, Prabowo WT, Vallejo R, van der Steen H, Vo K, Waldbieser G, Wang H, Wang X, Xiang J, Yang Y, Yant R, Yuan Z, Zeng Q, Zhou T (2017) Aquaculture genomics, genetics and breeding in the United States: current status, challenges, and priorities for future research. BMC Genomics 18:191

Adelman K, Marr MT, Werner J, Saunders A, Ni Z, Andrulis ED, Lis JT (2005) Efficient release from promoter-proximal stall sites requires transcript cleavage factor TFIIS. Mol Cell 17:103–112

Alcivar-Warren A, Meehan-Meola D, Park SW, Xu Z, Delaney M, Zuniga G (2007) ShrimpMap: a low-density, microsatellite-based

linkage map of the pacific whiteleg shrimp, *Litopenaeus vannamei*: identification of sex-linked markers in linkage group. J Shellfish Res 26:1259–1277

Andriantahina F, Liu XL, Huang H (2013) Genetic map construction and quantitative trait locus (QTL) detection of growth-related traits in *Litopenaeus vannamei* for selective breeding applications. PLoS One 8:e75206

Baird NA, Etter PD, Atwood TS, Currey MC, Shiver AL, Lewis ZA, Selker EU, Cresko WA, Johnson EA (2008) Rapid SNP discovery and genetic mapping using sequenced RAD markers. PLoS One 3: e3376

Berthier-Schaad Y, Kao WH, Coresh J, Zhang L, Ingersoll RG, Stephens R, Smith MW (2007) Reliability of high-throughput genotyping of whole genome amplified DNA in SNP genotyping studies. Electrophoresis 28:2812–2817

Bolger AM, Lohse M, Usadel B (2014) Trimmomatic: a flexible trimmer for Illumina sequence data. Bioinformatics 30:2114–2120

Bourgeois YX, Lhuillier E, Cézard T, Bertrand JA, Delahaie B, Cornuault J, Duval T, Bouchez O, Milá B, Thébaud C (2013) Mass production of SNP markers in a nonmodel passerine bird through RAD sequencing and contig mapping to the zebra finch genome. Mol Ecol Resour 13:899–907

Blagoev B, Ong SE, Kratchmarova I, Mann M (2004) Temporal analysis of phosphotyrosine-dependent signaling networks by quantitative proteomics. Nat Biotechnol 22:1139–1145

Catchen J, Hohenlohe PA, Bassham S, Amores A, Cresko WA (2013) Stacks: an analysis tool set for population genomics. Mol Ecol 22: 3124–3140

Carney JP, Maser RS, Olivares H, Davis EM, Le Beau M, Yates JR 3rd, Hays L, Morgan WF, Petrini JH (1998) The hMre11/hRad50 protein complex and Nijmegen breakage syndrome: linkage of double-strand break repair to the cellular DNA damage response. Cell 93: 477–486

Choi SH, Chung AR, Kang W, Park JY, Lee MS, Hwang SW, Kim DY, Kim SU, Ahn SH, Kim S, Han KH (2014) Silencing of hypoxia-inducible factor-1β induces anti-tumor effects in hepatoma cell lines under tumor hypoxia. PLoS One 9:e103304

Chuang SM, Madura K (2005) Saccharomyces cerevisiae Ub-conjugating enzyme Ubc4 binds the proteasome in the presence of translationally damaged proteins. Genetics 171:1477–1484

Cross TG, Scheel-Toellner D, Henriquez NV, Deacon E, Salmon M, Lord JM (2000) Serine/threonine protein kinases and apoptosis. Exp Cell Res 256:34–41

Dai X, Wang T, Gonzalez G, Wang Y (2018) Identification of YTH domain-containing proteins as the readers for N1-methyladenosine in RNA. Anal Chem 90:6380–6384

Das S, Upadhyaya HD, Bajaj D, Kujur A, Badoni S, Laxmi KV, Tripathi S, Gowda CL, Sharma S, Singh S, Tyagi AK, Parida SK (2015) Deploying QTL-seq for rapid delineation of a potential candidate gene underlying major trait-associated QTL in chickpea. DNA Res 22:193–203

de Vries MS, Webb SJ, Tu J, Cory E, Morgan V, Sah RL, Deheyn DD, Taylor JR (2016) Stress physiology and weapon integrity of intertidal mantis shrimp under future ocean conditions. Sci Rep 6:38637

Deng CX, Brodie SG (2000) Roles of BRCA1 and its interacting proteins. Bioessays 22:728–737

Du ZQ, Ciobanu DC, Onteru SK, Gorbach D, Mileham AJ, Jaramillo G, Rothschild MF (2010) A gene-based SNP linkage map for pacific white shrimp, *Litopenaeus vannamei*. Anim Genet 41:286–294

FAO (2012) Fisheries and Aquaculture Department: the state of world fisheries and aquaculture. Food and Agriculture Organization of the United Nations, Rome, Italy, p 37

Fehsenfeld S, Kiko R, Appelhans Y, Towle D, Zimmer M, Melzner F (2011) Effects of elevated seawater pCO2 on gene expression patterns in the gills of the green crab, *Carcinus maenas*. BMC Genomics 12:488

Fu B, Liu H, Yu X, Tong J (2016) A high-density genetic map and growth related QTL mapping in bighead carp (*Hypophthalmichthys nobilis*). Sci Rep 6:28679

Geng X, Liu S, Yao J, Bao L, Zhang J, Li C, Wang R, Sha J, Zeng P, Zhi D, Liu Z (2016) A genome-wide association study identifies multiple regions associated with head size in catfish. G3 (Bethesda) 6: 3389–3398

Goto Y, Hattori A, Ishii Y, Mizutani S, Tsujimoto M (2006) Enzymatic properties of human aminopeptidase a. regulation of its enzymatic activity by calcium and angiotensin IV. J Biol Chem 281:23503–23513

Groisman R, Polanowska J, Kuraoka I, Sawada J, Saijo M, Drapkin R, Kisselev AF, Tanaka K, Nakatani Y (2003) The ubiquitin ligase activity in the DDB2 and CSA complexes is differentially regulated by the COP9 signalosome in response to DNA damage. Cell 113: 357–367

Horne I, Haritos VS, Oakeshott JG (2009) Comparative and functional genomics of lipases in holometabolous insects. Insect Biochem Mol Biol 39:547–567

Huang W, Ren C, Li H, Huo D, Wang Y, Jiang X, Tian Y, Luo P, Chen T, Hu C (2017) Transcriptomic analyses on muscle tissues of *Litopenaeus vannamei* provide the first profile insight into the response to low temperature stress. PLoS One 12:e0178604

Huang W, Li H, Cheng C, Ren C, Chen T, Jiang X, Cheng K, Luo P, Hu C (2018) Analysis of the transcriptome data in *Litopenaeus vannamei* reveals the immune basis and predicts the hub regulation-genes in response to high-pH stress. PLoS One 13:e0207771

Ichikawa Y, Bayeva M, Ghanefar M, Potini V, Sun L, Mutharasan RK, Wu R, Khechaduri A, Jairaj Naik T, Ardehali H (2012) Disruption of ATP-binding cassette B8 in mice leads to cardiomyopathy through a decrease in mitochondrial iron export. Proc Natl Acad Sci U S A 109:4152–4157

Imprialou M, Petretto E, Bottolo L (2017) Expression QTLs mapping and analysis: a Bayesian perspective. Methods Mol Biol 1488:189–215

Jansen RC, Stam P (1994) High resolution of quantitative traits into multiple loci via interval mapping. Genetics 136:1447–1455

Kang HS, Beak JY, Kim YS, Petrovich RM, Collins JB, Grissom SF, Jetten AM (2006) NABP1, a novel RORgamma-regulated gene encoding a single-stranded nucleic-acid-binding protein. Biochem J 397:89–99

Kong S, Ke Q, Chen L, Zhou Z, Pu F, Zhao J, Bai H, Peng W, Xu P (2019) Constructing a high-density genetic linkage map for large yellow croaker (*Larimichthys crocea*) and mapping resistance trait against ciliate parasite *Cryptocaryon irritans*. Mar Biotechnol 21: 262–275

Kujur A, Upadhyaya HD, Shree T, Bajaj D, Das S, Saxena MS, Badoni S, Kumar V, Tripathi S, Gowda CL (2015) Ultra-high density intraspecific genetic linkage maps accelerate identification of functionally relevant molecular tags governing important agronomic traits in chickpea. Sci Rep 5:9468

Li C, Chen J (2008) The immune response of white shrimp *Litopenaeus vannamei* and its susceptibility to *Vibrio alginolyticus* under low and high pH stress. Fish Shellfish Immun 25:701–709

Li E, Chen L, Zeng C, Chen X, Yu N, Lai Q, Qin JG (2007) Growth, body composition, respiration and ambient ammonia nitrogen tolerance of the juvenile white shrimp, *Litopenaeus vannamei*, at different salinities. Aquaculture 265:385–390

Li J, Pu L, Han M, Zhu M, Zhang R, Xiang Y (2014) Soil salinization research in China: advances and prospects. J Geogr Sci 24:943–960

Li HL, Gu XH, Li BJ, Chen CH, Lin HR, Xia JH (2017) Genome-wide QTL analysis identified significant associations between hypoxia tolerance and mutations in the GPR132 and ABCG4 genes in Nile Tilapia. Mar Biotechnol 19:441–453

Li BJ, Zhu ZX, Gu XH, Lin HR, Xia JH (2019) QTL mapping for red blotches in Malaysia red tilapia (*Oreochromis spp.*). Mar Biotechnol 21:384–395

Liang L, Ren B, Chang Y, Tang R, Zhang L (2013) Inland brackish (saline-alkaline) water resources and fisheries utilization in China. Chin Fish Econ 31:138–145 (In China)

Lien S, Gidskehaug L, Moen T, Hayes BJ, Berg PR, Davidson WS, Omholt SW, Kent MP (2011) A dense SNP-based linkage map for Atlantic salmon (*Salmo salar*) reveals extended chromosome homeologies and striking differences in sex-specific recombination patterns. BMC Genomics 12:615

Lin X, Taguchi A, Park S, Kushner JA, Li F, Li Y, White MF (2004) Dysregulation of insulin receptor substrate 2 in beta cells and brain causes obesity and diabetes. J Clin Invest 114:908–916

Linley AJ, Mathieu MG, Miles AK, Rees RC, McArdle SE, Regad T (2012) The helicase HAGE expressed by malignant melanoma-initiating cells is required for tumor cell proliferation in vivo. J Biol Chem 287:13633–13643

Liu C, Wang J, Zhang Y, Liu L (2008) Effects of salinity and Na+/K+ in percolating water from saline-alkali soil on the growth of *Litopenaeus vannamei*. Chin J Appl Ecol 19:1337–1342 (In China)

Liu Y, Fang H, Lai Q, Liang L (2016) The current state and development strategy for China's saline-alkaline fisheries. Eng Sci CAE 18:74–78 (In China)

Liu H, Fu B, Me P, Feng X, Yu X, Tong J (2017) A high-density genetic linkage map and QTL fine mapping for body weight in crucian carp (*Carassius auratus*) using 2b-rad sequencing. G3 (Bethesda) 7: 2473–2487

Livak K, Schmittgen T (2001) Analysis of relative gene expression data using real-time quantitative PCR and the $2^{-\Delta\Delta CT}$ method. Methods 25:402–408

Louro B, Kuh H, Tine M, de Koning DJ, Batargias C, Volckaert FAM, Reinhardt R, Canario AVM, Deborah M (2016) Power characterization and refinement of growth related quantitative trait loci in European sea bass (*Dicentrarchus labrax*) using a comparative approach. Aquaculture 455:8–21

Lu X, Luan S, Hu LY, Mao Y, Tao Y, Zhong SP, Kong J (2016) High-resolution genetic linkage mapping, high-temperature tolerance and growth-related quantitative trait locus (QTL) identification in *Marsupenaeus japonicas*. Mol Gen Genomics 291:1391–1405

Luan Z, Pan L, Dong S (2003) A study of the culture technology of shrimp in low-lying soline-alkali soil along the yellow river. Chin J Oceanol Limn 3:71–77 (In China)

MacFarlane AW 4th, Yamazaki T, Fang M, Sigal LJ, Kurosaki T, Campbell KS (2008) Enhanced NK-cell development and function in BCAP-deficient mice. Blood 112:131–140

Malkowska M, Kokoszynska K, Rychlewski L, Wyrwicz L (2013) Structural bioinformatics of the general transcription factor TFIID. Biochimie 95:680–691

Márquez J, Olaso E (2014) Role of discoidin domain receptor 2 in wound healing. Histol Histopathol 29:1355–1364

Miller MR, Dunham JP, Amores A, Cresko WA, Johnson EA (2007) Rapid and cost-effective polymorphism identification and genotyping using restriction site associated. DNA (RAD) Markers 17:240–248

Ouellette LA, Reid RW, Blanchard SG, Brouwer CR (2018) LinkageMapView—rendering high-resolution linkage and QTL maps. Bioinformatics 34:306–307

Peterson BK, Weber JN, Kay EH, Fisher HS, Hoekstra HE (2012) Double digest RADseq: an inexpensive method for de novo SNP discovery and genotyping in model and non-model species. PLoS One 7: e37135

Piepho HP (2001) A quick method for computing approximate thresholds for quantitative trait loci detection. Genetics 157:425–432

Roggatz C, Lorch M, Hardege J, Benoit D (2016) Ocean acidification affects marine chemical communication by changing structure and function of peptide signaling molecules. Glob Change Biol 22: 3914–3926

Rowe HC, Renaut S, Guggisberg A (2011) RAD in the realm of next generation sequencing technologies. Mol Ecol 20:3499–3502

Seo M, Peeters AJ, Koiwai H, Oritani T, Marion-Poll A, Zeevaart JA, Koornneef M, Kamiya Y, Koshiba T (2000) The Arabidopsis aldehyde oxidase 3 (AAO3) gene product catalyzes the final step in abscisic acid biosynthesis in leaves. Proc Natl Acad Sci U S A 97: 12908–12913

Separovic D, Hanada K, Maitah MY, Nagy B, Hang I, Tainsky MA, Kraniak JM, Bielawski J (2007) Sphingomyelin synthase 1 suppresses ceramide production and apoptosis post-photodamage. Biochem Biophys Res Commun 358:196–202

Shao C, Niu Y, Rastas P, Liu Y, Xie Z, Li H, Wang L, Jiang Y, Tai S, Tian Y, Sakamoto T, Chen S (2015) Genome-wide SNP identification for the construction of a high-resolution genetic map of Japanese flounder (*Paralichthys olivaceus*): applications to QTL mapping of *Vibrio anguillarum* disease resistance and comparative genomic analysis. DNA Res 22:161–170

Stam P (1993) Construction of integrated genetic linkage maps by means of a new computer package: JoinMap. Plant J 3:739–744

Stölting KN, Nipper R, Lindtke D, Caseys C, Waeber S, Castiglione S, Lexer C (2013) Genomic scan for single nucleotide polymorphisms reveals patterns of divergence and gene flow between ecologically divergent species. Mol Ecol 22:842–855

Soñanez-Organis JG, Peregrino-Uriarte AB, Gómez-Jiménez S, López-Zavala A, Forman HJ, Yepiz-Plascencia G (2009) Molecular characterization of hypoxia inducible factor-1 (HIF-1) from the white shrimp *Litopenaeus vannamei* and tissuespecific expression under hypoxia. Comp Biochem Physiol C Toxicol Pharmacol 150:395–405

Sun X, Liu D, Zhang X, Li W, Liu H, Hong W, Jiang C, Guan N, Ma C, Zeng H, Xu C, Song J, Huang L, Wang C, Shi J, Wang R, Zheng X, Lu C, Wang X, Zheng H (2013) SLAF-seq: an efficient method of large-scale denovo SNP discovery and genotyping using high-throughput sequencing. PLoS One 8:e58700

Sun C, Niu Y, Ye X, Dong J, Hu W, Zeng Q, Chen Z, Tian Y, Zhang J, Lu M (2017) Construction of a high-density linkage map and mapping of sex determination and growth-related loci in the mandarin fish (*Siniperca chuatsi*). BMC Genomics 18:446

Tong JG, Sun XW (2015) Genetic and genomic analyses for economically important traits and their applications in molecular breeding of cultured fish. Science China-Life Sci 58:178–186

Toulany M, Rodemann HP (2015) Phosphatidylinositol 3-kinase/Akt signaling as a key mediator of tumor cell responsiveness to radiation. Semin Cancer Biol 35:180–190

van Daal A, Elgin SC (1992) A histone variant, H2AvD, is essential in *Drosophila melanogaster*. Mol Biol Cell 3:593–602

Van Ooijen JW (2011) Multipoint maximum likelihood mapping in a full-sib family of an out breeding species. Genet Res 93:343–349

van Wijk SJ, Timmers HT (2010) The family of ubiquitin-conjugating enzymes (E2s): deciding between life and death of proteins. FASEB J 24:981–993.

Wan SM, Liu H, Zhao BW, Nie CH, Wang WM, Gao ZX (2017) Construction of a high-density linkage map and fine mapping of QTLs for growth and gonad related traits in blunt snout bream. Sci Rep 7:46509

Wang PY, Weng J, Anderson RG (2005) OSBP is a cholesterol-regulated scaffolding protein in control of ERK 1/2 activation. Science 307: 1472–1476

Wang WN, Zhou J, Wang P, Tian TT, Zheng Y, Liu Y, Mai WJ, Wang AL (2009) Oxidative stress, DNA damage and antioxidant enzyme gene expression in the Pacific white shrimp, *Litopenaeus vannamei* when exposed to acute pH stress. Comp Biochem Phys C 150:428–435

Wang S, Meyer E, McKay JK, Matz MV (2012) 2b-RAD: a simple and flexible method for genome-wide genotyping. Nat Methods 9:808–810

Wang J, Luo MC, Chen Z, You FM, Wei Y, Zheng Y, Dvorak J (2013a) *Aegilops tauschii* single nucleotide polymorphisms shed light on the origins of wheat genome genetic diversity and pinpoint the geographic origin of hexaploid wheat. New Phytol 198:925–937

Wang X, Li E, Xiong Z, Chen K, Yu N, Du Z, Chen L (2013b) Low salinity decreases the tolerance to two pesticides, beta-cypermethrin and acephate, of whiteleg shrimp, *Litopenaeus vannamei*. J Aquac Res Development 4:190

Wang S, Feng Q, Zhou Y, Mao X, Chen Y, Xu H (2017) Dynamic changes in water and salinity in saline-alkali soils after simulated irrigation and leaching. PLoS One 12:e0187536

Wang X, Fu B, Yu X, Qu C, Zhang Q, Tong J (2018) Fine mapping of growth-related quantitative trait loci in Yellow River carp (*Cyprinus carpio haematoperus*). Aquaculture 484:277–285

Watt MJ, Spriet LL (2010) Triacylglycerol lipases and metabolic control: implications for health and disease. Am J Physiol Endocrinol Metab 299:E162–E168

Wu F, Wang T, Cui S, Xie Z, Dupont S, Zeng J, Gu H, Kong H, Hu M, Lu W, Wang Y (2017) Effects of seawater pH and temperature on foraging behavior of the Japanese stone crab *Charybdis japonica*. Mar Pollut Bull 120:99–108

Xu J, Zhao Z, Zhang X, Zheng X, Li J, Jiang Y, Kuang Y, Zhang Y, Feng J, Li C, Yu J, Li Q, Zhu Y, Liu Y, Xu P, Sun X (2014) Development and evaluation of the first high-throughput SNP array for common carp (*Cyprinus carpio*). BMC Genomics 15:307

Xue M (2018) Experiment and analysis of pond ecological farming technique in salt and alkaline soil of the yellow river beach. Shaanxi Water Resources 1:88–96 (In China)

Yu Y, Zhang X, Yuan J, Li F, Chen X, Zhao Y, Huang L, Zheng H, Xiang J (2015) Genome survey and high-density genetic map construction provide genomic and genetic resources for the Pacific White Shrimp *Litopenaeus vannamei*. Sci Rep 5:15612

Yu Y, Wang Q, Zhang Q, Luo Z, Wang Y, Zhang X, Huang H, Xiang J, Li F (2019) Genome scan for genomic regions and genes associated with growth trait in pacific white shrimp *Litopeneaus vannamei*. Mar Biotechnol 21:374–383

Yue GH (2014) Recent advances of genome mapping and marker-assisted selection in aquaculture. Fish Fish 15:376–396

Zhang D (2016) Technology for healthily breeding *Penaeus vannamei* boone in saline-alkali land of our country's northern region. Shanxi Hydrotechnics 4:127–128 (In China)

Zhang G, Zhang X, Ye H, Jiang S, Yu H, Li J, Shi Q, Chen G, Zhou Z, Luo J, You X (2018) Construction of high-density genetic linkage maps and QTL mapping in the golden pompano. Aquaculture 482: 90–95

Zhang X, Yuan J, Sun Y, Li S, Gao Y, Yu Y, Liu C, Wang Q, Lv X, Zhang X, Ma KY, Wang X, Lin W, Wang L, Zhu X, Zhang C, Zhang J, Jin S, Yu K, Kong J, Xu P, Chen J, Zhang H, Sorgeloos P, Sagi A, Alcivar-Warren A, Liu Z, Wang L, Ruan J, Chu KH, Liu B, Li F, Xiang J (2019) Penaeid shrimp genome provides insights into benthic adaptation and frequent molting. Nat Commun 10:356

Zimmerman SW, Yi YJ, Sutovsky M, van Leeuwen FW, Conant G, Sutovsky P (2014) Identification and characterization of RING-finger ubiquitin ligase UBR7 in mammalian spermatozoa. Cell Tissue Res 356:261–278